IRAQI BULLETIN OF GEOLOGY AND MINING (IBGM)\
IRAQ GEOLOGICAL SURVEY (GEOSURV-IRAQ)

*IBGM (**2025**, Vol 21; Issue 2)* *545-572*

PETROPHYSICAL EVALUATION OF THE PALEOGENE KHURMALA AND AVANAH FORMATIONS FROM A SELECTED WELL IN THE KHURMALA OILFIELD, NORTHERN IRAQ

Shiraz K. Birezhy[1] and Dler H. Baban[2*]

[1] Department of Earth Sciences and Petroleum, University of Salahaddin, Erbil, Iraq; shirazkafi@gmail.com
[2] Department of Earth Sciences and Petroleum, University of Sulaimani, Sulaimaniyah, Iraq; dler.mohamad@univsul.edu.iq
***** Correspondence: dler.mohamad@univsul.edu.iq, Dler H. Baban (ORCID, 0000-0001-9619-162X)

Type of the Paper (Article)
Received: 17/05/2025
Accepted: 26/10/2025
Available online: 27/12/2025

Abstract

The Paleogene Avanah and Khurmala formations were investigated from a reservoir characterization point of view from a selected well (KX) in the Khurmala Oilfield, northern Iraq. The conventional wireline log data were used to determine the petrophysical properties and reservoir quality of the studied formations. The common lithology of both formations is identified based on porosity log data and utilizing density versus neutron and M-N crossplots. The upper part of the Avanah Formation, informally known as Avanah Dense, is composed of clean limestone and dolomitic limestone, whereas the lower part of the formation, known informally as Avanah Porous, is composed mainly of dolostone, limedolostone, and limestone with different ratios of shale content. Dolostone and limedolostone comprise most parts of the Khurmala Formation, with shaly and shale intervals at different parts of the formation. The shale volume has been determined using the data from the gamma ray log. The shale in the Avanah Porous and the Khurmala Formation is distributed in a laminated mode in addition to the dispersed and less frequent structural mode. Porosity was calculated for the studied formations using the recorded data of the sonic, density, and neutron logs and corrected for shale impact. The average neutron-density combination porosity of the Avanah Dense is about 10.7%, the Avanah Porous 24.36%, and about 24.56% in the Khurmala Formation. Permeable zones with a few thousand millidarcies are common in the Avanah Porous and in the Khurmala Formation, whereas tight horizons and zones of relatively low permeability are intercalated zones with a few hundred millidarcies in the Avanah Dense. Hydrocarbons in different ratios exist within the entire studied section. The Khurmala Formation is divided into two reservoir units, while the Avanah Formation is divided into six reservoir units based on differences in shale volume, porosity, permeability, and water saturation. Flow zone indicator and movable hydrocarbon index methods were used to determine the flow capacity of the identified reservoir units and the hydrocarbon movability within each unit.

ISSN 1811-4539, EISSN 3005-3714
https://doi.org/10.59150/ibgm2102a29
IBGM: http://ibgm-iq.org/
Academic Scientific Journals: www.iasj.net

Keywords: Avanah Formation; Khurmala Formation; Reservoir Characterization; Hydrocarbon Movable Index; Flow Zone Indicator.

1. Introduction

Reservoir characterization is a comprehensive process that involves gathering and analyzing critical information about the distribution and properties of a reservoir. This process is essential for understanding the reservoir's heterogeneity, which refers to the variations in its composition by examining factors such as rock types, fluid properties, and pore spaces, and petrophysical properties of the reservoir, including porosity, permeability, and saturation (Aminzadeh & Dasgupta, 2013).

Formation evaluation, or reservoir characterization, includes various techniques and tools that can collectively enhance reservoir assessments. The evaluation generally considers both the reservoir rock and the nature and volume of the fluid content. The primary reservoir parameters representing the evaluation's goal are porosity, permeability, and fluid saturations. Other important parameters may involve capillary pressures, wettability, and fluid compositions, in addition to assessing the movability of hydrocarbons and the ease with which they can be produced.

The most significant kind of hydrocarbon reserves is carbonate deposits. Akbar et al. (2000) assessed that carbonate reservoirs contain roughly 60% of the world's oil reserves. According to Schlumberger (2019), carbonate reservoirs contain 70% of the Middle East's conventional oil reserves. Compared to sandstone reservoirs, this kind of reservoir may be thought to be more diverse; this is particularly true if one looks at its most crucial attribute, which is dual or even multiple porosity (permeability; Kargarpour, 2020).

The Paleocene – Early Eocene Khurmala and Avanah formations, of a carbonate nature, are among the most desirable targets of the majority of petroleum exploration operations carried out in northern Iraq, particularly in Kirkuk and the surrounding areas.

The main aim of this study is to assess the petrophysical properties of the Khurmala and Avanah formations in a selected well from the Khurmala Oilfield located in northern Iraq. Additionally, it aims to characterize their reservoir quality based on the available wireline log data.

2. Study Area

The Khurmala Oilfield is generally considered the third dome of the supergiant Kirkuk Oilfield towards its northwestern plunge. Two of the three domes of the Kirkuk structure (Baba and Avanah) are geographically located in Kirkuk Governorate, while the Kurmala dome is related to the Erbil Governorate, and it's about 34 km to the west of Erbil City (Figure 1).

The Khurmala dome is separated from the Kirkuk Oilfield’s middle dome, Avanah, by the Debaga saddle. The length of the Khurmala dome is about 20 km, and its width is about 3.5 km

(NOC, 1994). According to the preliminary estimations, the Kurmala Oilfield contains a gas cap in addition to an oil column of about 104 m height (NOC, 1994).

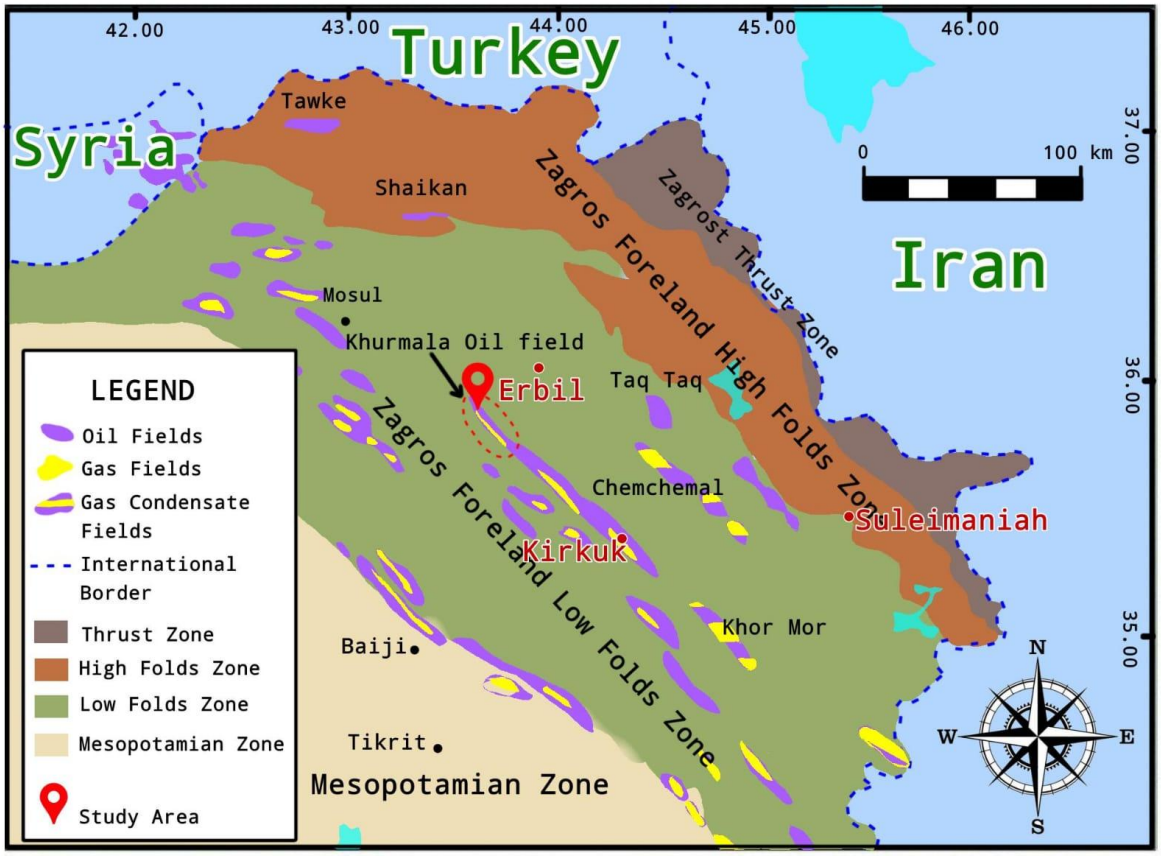

Figure 1. Location of the Khurmala (Dome) Oilfield at the northwestern end of the Kirkuk Oilfield plotted on the tectonic map of Iraq.

3. Studied Formations

3.1 Avanah Formation

Bellen et al. (1959) state that McGinty initially characterized the formation in 1953 from the Kirkuk 116 well, which is situated on the Avanah dome of the Kirkuk anticline in the Foothill Zone, where the formation has been penetrated between depths of 672.3 and 883.8 m with a true thickness of 212m.

The formation is an example of the second neritic, shoal-type limestone unit from the late Lower Eocene/Upper Eocene Cycle, which in its type section consists of limestones that are typically dolomitized and recrystallized (Bellen et al., 1959)

According to Jassim & Buday (2006), during the period of high sea level, the Avanah Formation was deposited along the northeast coast of the basin as an isolated carbonate shoal connected to a paleoridge. A transgression is most likely associated with the sudden transition from the

lagoonal facies of the Khurmala Formation to the shoal facies of the Avanah Formation (Bellen et al., 1959).

The lithostratigraphy and lithofacies of the formation were investigated by a number of authors in outcrop and subsurface sections in northern Iraq (Sharbazheri & Abawi, 1987; Aziz, 2012; Al-Hamdany & Sulaiman, 2014; Barzani, 2016; Abdullah et al., 2020; Musheer, 2021; Asaad, 2022; Asaad et al., 2022; Mamaseni et al., 2024)

It is important to mention that lately the formation has been informally divided into two distinctive parts by the petroleum companies when characterizing the Avanah Formation. The upper part is called Avanah Dense due to being of lower porosity and permeability compared to the lower part, which they used to name the Avanah Porous

3.2. Khurmala Formation

The Khurmal Formation was first reported by Bellen in 1953 from the well K-114 between drilled depths 983.2 and 1176 m and approximately 185 m true thickness (Bellen et al., 1959). The lithology of the formation generally consists of dolostone and finely recrystallized limestone with an occasional occurrence of secondary anhydrites. The formation, as stated by Bellen et al. (1959), is of Paleocene - Early Eocene age without support from any fossil evidence but based mainly on stratigraphic arguments, and they considered the Kurmala Formation as the lagoonal equivalent of the Sinjar Formation. Aqrawi et al. (2010) stated that the lagoonal conditions in which the Khurmala Formation was deposited were subsequently initiated behind the platform margin barrier, where the Sinjar Formation was deposited. The formation is only found in a belt that runs from the Chemchemal-Qizl Dagh to the NE to Jabal Maqlob to the NW (Jassim & Buday, 2006).

The Khurmala Formation has been the subject of numerous studies that examine its petrography, stratigraphy, depositional environments, and fossil content (Al-Eisa, 1983; Al-Barzanji, 1989; Al-Qayim, 1995; Al-Banna et al., 2006; Khalaf & Aziz, 2009; Karim, 2009; Al-Dabagh, 2010; Al-Lihaibi, 2012; Al-Ehmeedy et al., 2012; Omer et al., 2014; Asaad & Balaky, 2018; Karim et al., 2018; Asaad et al., 2022; Ahmed, 2022; Abid et al., 2023).

The petrophysical properties of the Khurmala Formation were investigated by a number of works in different locations of the Kurdistan Region at the northern part of Iraq (Barzani & Al-Qayim, 2019; Rashid et al., 2020; Abdula et al., 2024).

4. Materials and methods

The data utilized for this study included the available conventional wireline logs of caliper, gamma-ray, spontaneous potential (SP), sonic, density, neutron, and resistivity logs. The log data covered the entire penetrated 128 m thick Avanah and Khurmala formations in well KX between drilled depths 811 and 1039 m.

The applied software in this study included NeuraLog, Techlog 64 version 2015.3, and Grapher version 18.

The methodology began with digitizing the logs using NeuraLog software and replotting them with appropriate scales. The details of the lithology were detected using the bulk density (ρb) - neutron porosity ($Ø_N$) crossplot from Schlumberger (1979). Applying Equations 1 and 2, the shale content of the investigated formations was determined using the gamma-ray log data.

$$IGr = (Grlog - Grmin)/(Grmax - Grmin) \quad (1)$$

$$Vsh = 0.083\ (2^{(3.7IGr)} - 1) \quad (2)$$

Where: IGr: Gamma ray index. Gr_{log}: Record of gamma ray at any depth. Gr_{min}: Recorded gamma ray in a clean zone. Gr_{max}: Recorded gamma ray in a shale zone. Vsh: Shale volume

The three porosity logs of sonic, density, and neutron were used to calculate the porosity of the formations under study. Sonic porosity ($Ø_S$) and density porosity ($Ø_D$) were calculated from the recorded interval transit time (Δt) of the sonic log and the ρb of the density log, respectively, using Equations 3 and 4.

$$ØS = (\Delta tlog - \Delta tmat)/(\Delta tfl - \Delta tmat) \quad (3)$$

$$ØD = (\rho mat - \rho b)/(\rho mat - \rho fl) \quad (4)$$

Where: $Ø_S$: Calculated porosity from the recorded data of the sonic log. Δt_{log}: Recorded interval transit time at any depth. Δt_{mat}: Interval transit time for the matrix. Δt_{fl}: Interval transit time for the filtrated fluid. $Ø_D$: Calculated porosity from the recorded data of the density log. ρ_{mat}: Density of the matrix. ρb: The recorded bulk density by the density log. ρ_{fl}: Density of the filtrated drilling mud

Before being used in further evaluation stages, the porosity values that were acquired from the porosity logs were corrected for the shale impact.

The calculations of the water and hydrocarbon saturations were done using data from the resistivity logs and applying Archie's proposed equations for the invaded and uninvaded zones (Equations 5 and 6, respectively).

$$Sw = \left[\frac{Rw\ a}{(ØNDcorr)^m\ Rt}\right]^{½} \quad (5)$$

$$Sxo = [\frac{Rmf\ a}{(\emptyset NDcorr)^m\ Rxo}]^{½} \quad (6)$$

Where: S_w: Water saturation in the uninvaded zone. R_w: Resistivity of the formation water.

a: Tortuosity factor (usually equals 1.0). $Ø_{NDcorr}$: Neutron-density combination corrected porosity. m: Cementation factor. R_t: True resistivity (resistivity of the uninvaded zone). n: Saturation exponent (usually equals 2.0). S_{xo}: Water saturation in the flushed zone. R_{mf}: Resistivity of the filtrated mud. R_{xo}: Resistivity of the flushed zone.

5. Results and discussion

The results obtained will be presented according to the steps followed in the reservoir characterizations based on wireline log data, along with a discussion of them.

5.1. Lithology identification

In addition to their main functions in providing porosity values, porosity logs are also very helpful in detecting the lithologies of the logged intervals.

When neutron and density logs are combined, their data will be more useful for lithology identification. The ρb–ØN and the M-N crossplots of Schlumberger are among the most applied methods for lithology identification using log data. Sandstone, limestone, dolomites, and even anhydrites are examples of lithologies that can be easily identified on such a crossplot by observing the type of drilling fluid (salt mud or fresh mud). Bateman (1985) identified the shale zone in the ρb – ØN crossplot as the area enclosed by ØN 30 – 40% and ρb 2.35 – 2.50gm/cc. Consequently, the sample points will be distorted toward the crossplot's right corner due to the influence of the shale content. Conversely, gas content will cause the readings to be distorted toward the top of the crossplot. Although this crossplot aids in identifying lithologies of the reservoir beds, but still difficult to distinguish complex lithologies with multiple mineralogy types (Halliburton, 2001).

Figure 2 shows the distribution of the sample points of the Avanah (dense and porous parts) and Khurmala formations in well KX on the ρb – ØN crossplot.

The dominant limestone lithology of the upper part of the Avanah Formation (Avanah Dense) is clear, with indications of occasional anhydritic lithology or anhydrite nodules (Figure 2a).

The pull-up of the sample points towards the sandstone field is most likely due to the effect of the gas rather than being a lithologic variation. Low shale content is expected for the Avanah Dense, as appears from the low values of the recorded gamma-ray log.

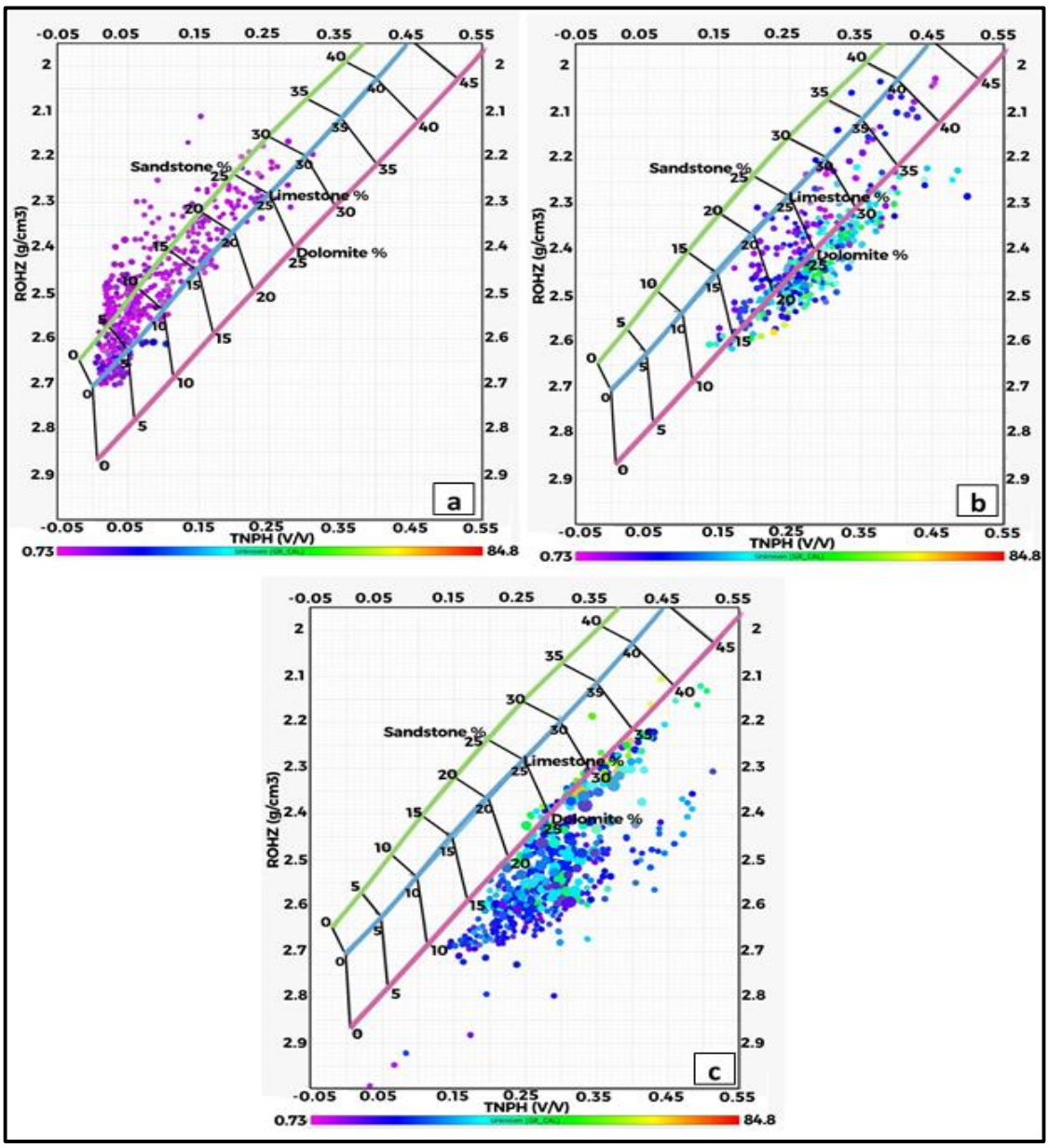

Figure 2. ρb-ØN crossplot for determining lithology for **a**, the upper part of the Avanah Formation (Avanah Dense); **b**, the lower part of the Avanah Formation (Avanah Porous); and **c**, the Khurmala Formation in well KX. The color of the sample points reflects the value of their gamma ray record.

The lower part of the Avanah Formation (Avanah Porous) consists mainly of dolostone and limedolostone (Figure 2b) and has a higher shale content than the upper part of the formation (Avanah Dense). This is indicated by the elevated values of the recorded gamma ray-log and the distortion of the sample points toward the shale region on the right side of the crossplot.

Khurmala Formation, as appeared from the distribution of its sample points on the crossplot (Figure 2c) composed mainly of dolostone with an expectation for the existence of appreciable percentages of shale, which may appear as part of an argillaceous limestone.

The distortion of the points towards the shale region of the crossplot is very obvious, which indicates the Khurmala Formation has higher shale content than both parts of the Avanah Formation.

For the identification of minerals with complex lithologies, the M-N cross plot, as illustrated by Schlumberger (Burke et al., 1969), is highly helpful. The lithology-dependent values M and N are obtained by combining the data from the three porosity logs of sonic, density, and neutron (Equations 7 and 8).

According to Burke et al. (1969), these are merely the slopes of the distinct lithology lines on the density-neutron and sonic-density cross plot charts, respectively.

$$SM = \frac{\Delta t_f - \Delta t}{\rho_b - \rho_f} \times 0.01 \quad (7)$$

$$N = \frac{\emptyset_{Nf} - \emptyset_N}{\rho_b - \rho_f} \quad (8)$$

$Ø_{Nf}$ for fresh mud is equal to 1.0.

The main type of rock, limestone, and the impact of the gas are easier to see when using the M – N method for the Avanah Dense (Figure 3a). The same applies to the dolostone and limedolostone rock types of the Avanah Porous, which have more shale (Figure 3b). Khurmala Formation and its dolostone lithology and the effect of the shale content are also detected by the M-N crossplot as they are by the ρb – ØN crossplot (Figure 3c).

5.2. Shale content

Shale content in reservoirs has a number of detrimental consequences, and the degree of those effects is significantly influenced by the composition, volume, and distribution of shale in the reservoir rock (Baban et al., 2023). The presence of clay-sized particles in a reservoir's rock negatively impacts its petrophysical characteristics by reducing the reservoir's effective and total porosities and, as a result, its permeability.

Shale content for the studied Avanah and Khurmala formations was calculated using the data from the gamma-ray log and applying Equation 1 along with the proposed Equation 2 by Larionov (1969) for shale calculation in unconsolidated Tertiary-age rocks (Figure 4).

The upper part of the Avanah Formation (Avanah Dense) appeared clean, with generally less than 10% shale content. In contrast, shaly intervals with shale contents between 10 and 35% (Ghorab et al., 2008) predominated in the middle and lower parts of the Avanah Porous, along

with a shale interval exceeding 35% shale content at the contact with the underlying Khurmala Formation for rocks containing more than 35% shale.

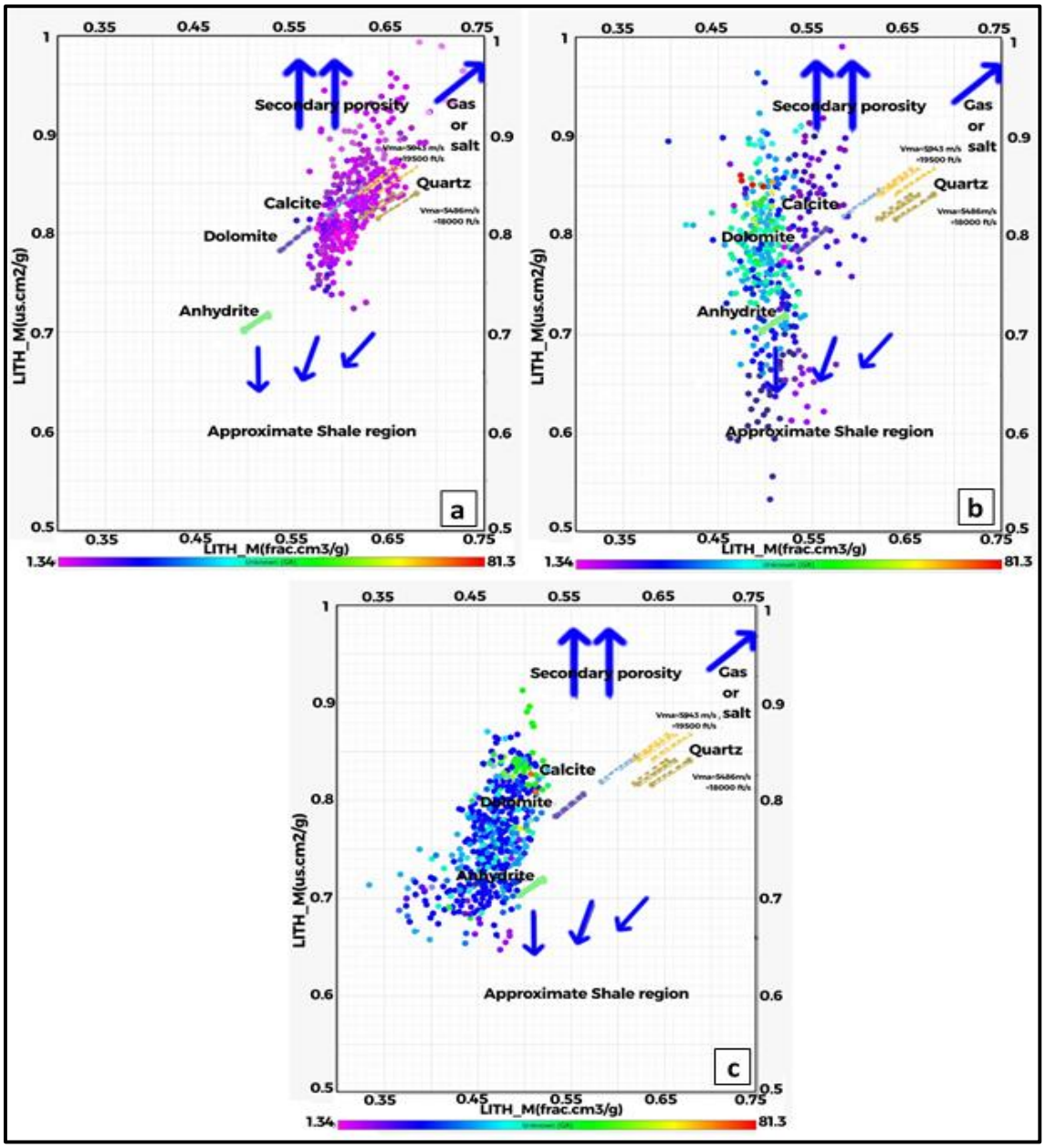

Figure 3. M-N crossplot for determining lithology for **a**, the upper part of the Avanah Formation (Avanah Dense); **b**, the lower part of the Avanah Formation (Avanah Porous); and **c**, the Khurmala Formation in well KX. The color of the sample points reflects the value of their gamma ray record.

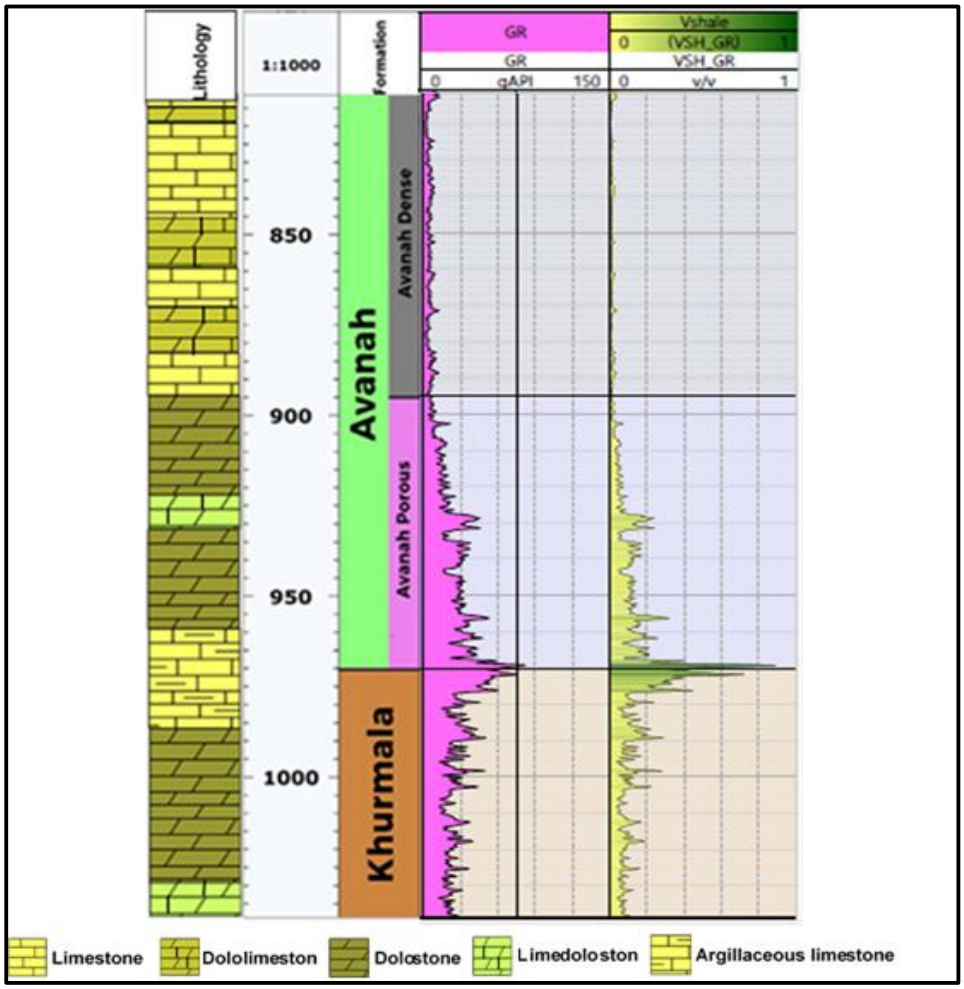

Figure 4. The gamma-ray record and the calculated shale volume for the upper and lower parts of the Avanah Formation (Avanah Dense and Avanah Porous) and the Khurmala Formation in well KX.

Most parts of the Khurmala Formation are shaly except its upper 15 m between depths 990 and 1005 m, which can be considered as a shale interval, and that is according to the standard proposed by.

Besides the effect of the shale volume, the mode by which the shale is distributed also affects the reservoir rock's properties. Thomas & Stieber (1975) used both ØN and ØD values to differentiate between the structural, laminated, and dispersed types of shale distribution within sandstone rocks.

The same idea was later applied to the carbonate reservoir rocks in a number of reservoir characterization works (Yang, 2015; Moradi et al., 2016; Baban et al., 2020; Baban & Ahmed, 2021).

The reservoir quality is impacted to varying degrees by each of the three shale dispersion patterns. The dispersed mode, which is the distribution of clay-sized particles between the grains, is the most effective in lowering the reservoir rock's porosity and permeability. Although the distribution of laminated shale also helps to reduce porosity and permeability, the most obvious effect is the development of vertical anisotropy in permeability (Baban et al., 2023).

Benthic microbial mats can produce wavy lamination in shale, bottom-flowing current deposition can provide thick lamination, while suspension settling can produce thin lamination (O'Brien, 1996). The porosity and permeability of the reservoir rock are known to be unaffected by the structural type of clay distribution, which involves replacing any rock grain with a shale grain.

The distribution modes for the shale in the studied Avanah Porous and the Khurmala Formation in well KX are shown in Figure 5. The very low shale content in the upper part of the Avanah Formation makes it unnecessary to determine the mode of shale distribution in the Avanah Dense. The shale in the Avanah Porous (Figure 5a) is mainly of a laminated mode of distribution and partially of a dispersed and structural mode. The Khurmala Formation is likewise the Avanah Porous, its shale content distributed largely in dispersed and laminated modes and less commonly in structural mode (Figure 5b). It's worth mentioning that the sample points of the Avanah Porous and the Khurmala Formation are located outside the established triangle, indicating the existence of gas or light oil, or, more specifically, a high bulk volume of gas or light oil.

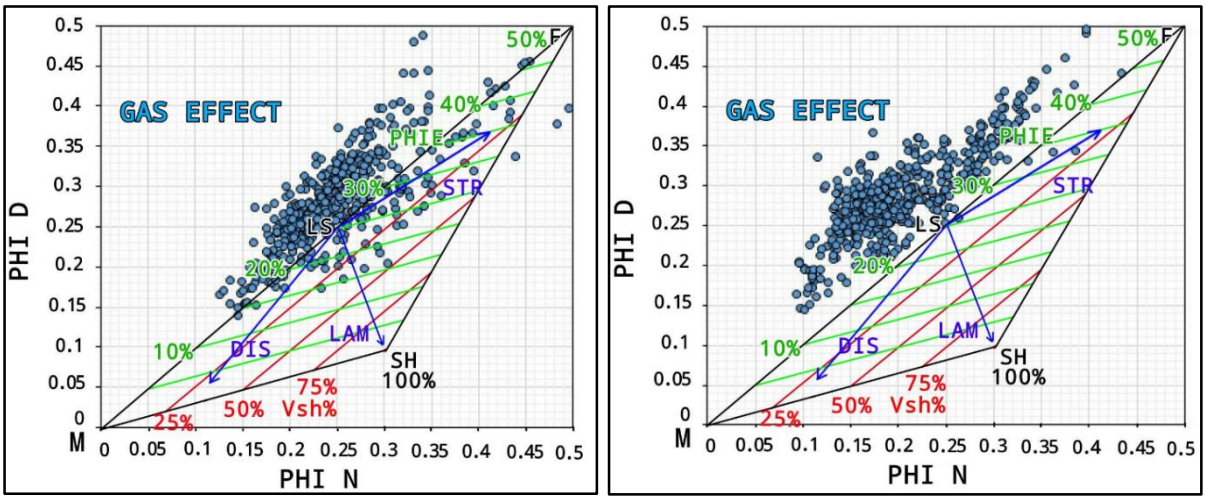

Figure 5. Shale distribution mode determination based on the Thomas-Stieber crossplot for **a**, Avanah Porous; and **b**, Khurmala Formation in well KX. (**M**, matrix **F**, fluid **SH**, shale **LM**, limestone **DIS**, dispersed **LAM**, laminated **STR**, structural).

5.3. Porosity calculation

The three porosity logs—sonic, density, and neutron—were available for the Avanah and Khurmala formations under investigation in this work. The recorded Δt of the sonic log and the ρb of the density log were converted to sonic porosity and density porosity, respectively, using equations 3 and 4. The calculated sonic and density porosities, along with the recorded neutron porosity, were corrected for the shale impact using equations 9-11proposed by Dewan (1983).

$$\emptyset_{Scorr} = \emptyset_S - V_{sh} * \emptyset_{Ssh} \quad (9)$$

$$\emptyset_{Dcorr} = \emptyset_D - V_{sh} * \emptyset_{Dsh} \quad (10)$$

$$\emptyset_{Ncorr} = \emptyset_N - V_{sh} * \emptyset_{Nsh} \quad (11)$$

Where: $Ø_{Scorr}$: Sonic log-derived porosity corrected for shale impact. $Ø_S$: Sonic log-derived porosity. $Ø_{Ssh}$: Sonic porosity for adjacent shale. V_{sh}: Volume of shale. $Ø_{Dcorr}$: Density log-derived porosity corrected for shale impact. $Ø_D$: Density log-derived porosity. $Ø_{Dsh}$: Density porosity for adjacent shale. $Ø_{Ncorr}$: Corrected neutron porosity from shale impact. $Ø_N$: Neutron log-derived porosity uncorrected for shale. $Ø_{Nsh}$: Neutron porosity for adjacent shale

Figure 6 shows the calculated corrected sonic, density, and neutron porosities along with the shale content for the Avanah and Khurmala formations in well KX.

For reservoir characterization, this study utilizes the calculated corrected neutron-density combination porosity ($Ø_{NDcorr}$), which represents the average of the corrected neutron porosity and corrected density porosity.

Most parts of the Avanah Dense have less than 10% porosity, intercalated occasionally by less than 2 m thick horizons of higher porosity. The exception is for the 20 m thick interval between depths 845 and 865 m, where porosities of about 20% can be seen.

The average porosity for the Avanah Dense in well KX is about 10.7% and qualitatively evaluated as good porosity according to the standard of porosity qualification of (North, 1985).

The lower part of the Avanah Formation (Avanah Porous) has porosities ranging mostly between 15 and 30%, with the existence of a few horizons of exceptionally high porosities exceeding 35%. The average porosity for the entire Avanah Porous well KX is about 24.38%, and it is considered very good porosity.

The Khurmala Formation, as appears in Figure 6, is almost of good to very good porosity, with around 20% in most parts. A few meters-thick horizons with higher than 30% porosity can also be observed in the formation, whose average porosity is around 24.54%.

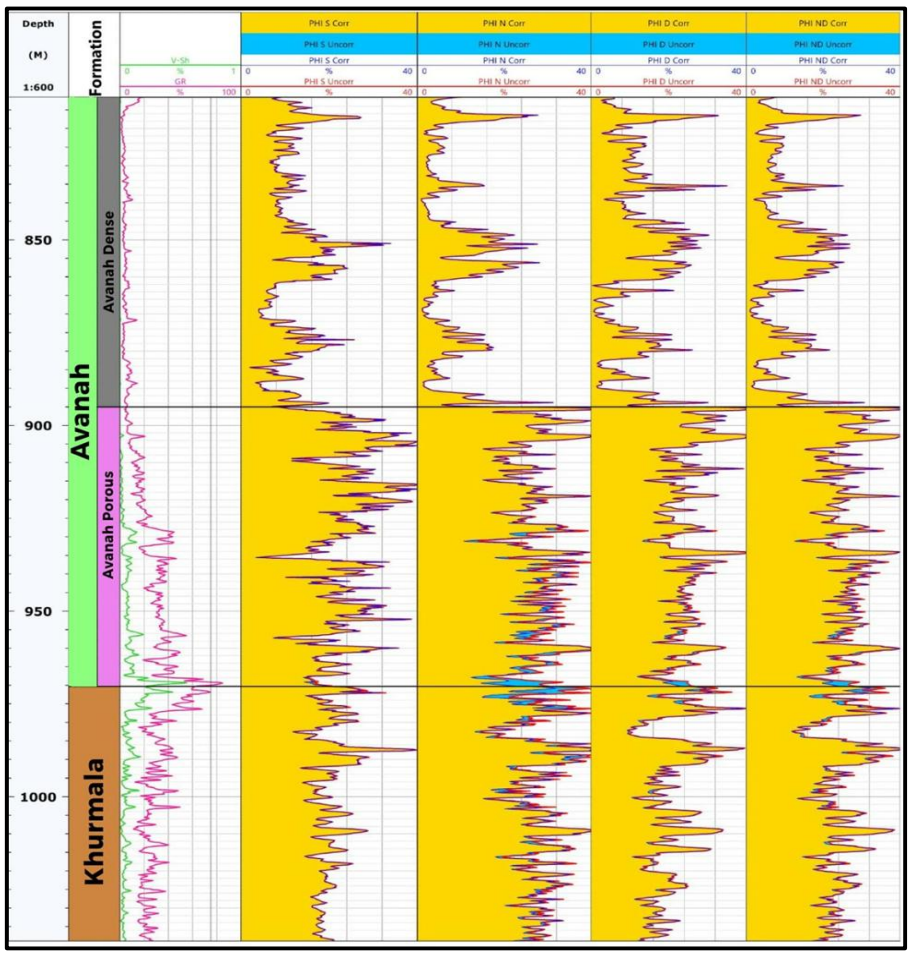

Figure 6. The calculated sonic, neutron, density, and neutron-density combination corrected porosities for the Avanah and Khurmala formations, along with their shale content in well KX.

While primary porosity refers to the intergranular pore spaces of the rock that occurred during the rock's deposition period, secondary porosity includes all additional porosities, such as fractures and vugs that formed during the various burial stages as a result of diagenesis processes and tectonic stresses (Schlumberger, 1989).

Finding fractured intervals in any reservoir is crucial, particularly for confined carbonate reservoirs. Fractures are particularly successful in creating channels for fluid to flow, which raises the permeability and production capacity even if they might not significantly increase the matrix porosity.

Finding intervals with secondary porosity (fracture porosity) is made easier with the use of the porosity data computed from the sonic log and the radiation tools of density and neutron logs by applying the simple equation 12.

$$\emptyset_{sec} = \emptyset_{NDcorr} - \emptyset_{Scorr} \tag{12}$$

Where: Θ_{sec}: Secondary porosity (fracture porosity). Θ_{NDcorr}: Corrected combination neutron - density porosity. Θ_{Scorr}: Corrected sonic porosity.

Secondary porosity has a different effect on sonic logs than on neutron and density logs. Sonic logging tools react mainly to intergranular porosity and mostly disregard vuggy porosity and fractures; neutron and density tools react to total porosity (Schlumberger, 1989).

The calculated secondary porosity for the Avanah and Khurmala formations in well KX (Figure 7) confirmed the effective role of secondary porosity, which may consist of fractures, in enhancing the total porosity of the lower part of the Avanah Formation (Avanah Porous) and the Khurmala Formation, while contributing less to the additional pore spaces in the upper part of the Avanah Formation (Avanah Dense). Generally, the secondary porosities comprise between 0.0% and about 10% of the total porosity of both formations, with a few exceptional zones exhibiting higher than 10% secondary porosity, especially in the Avanah Porous.

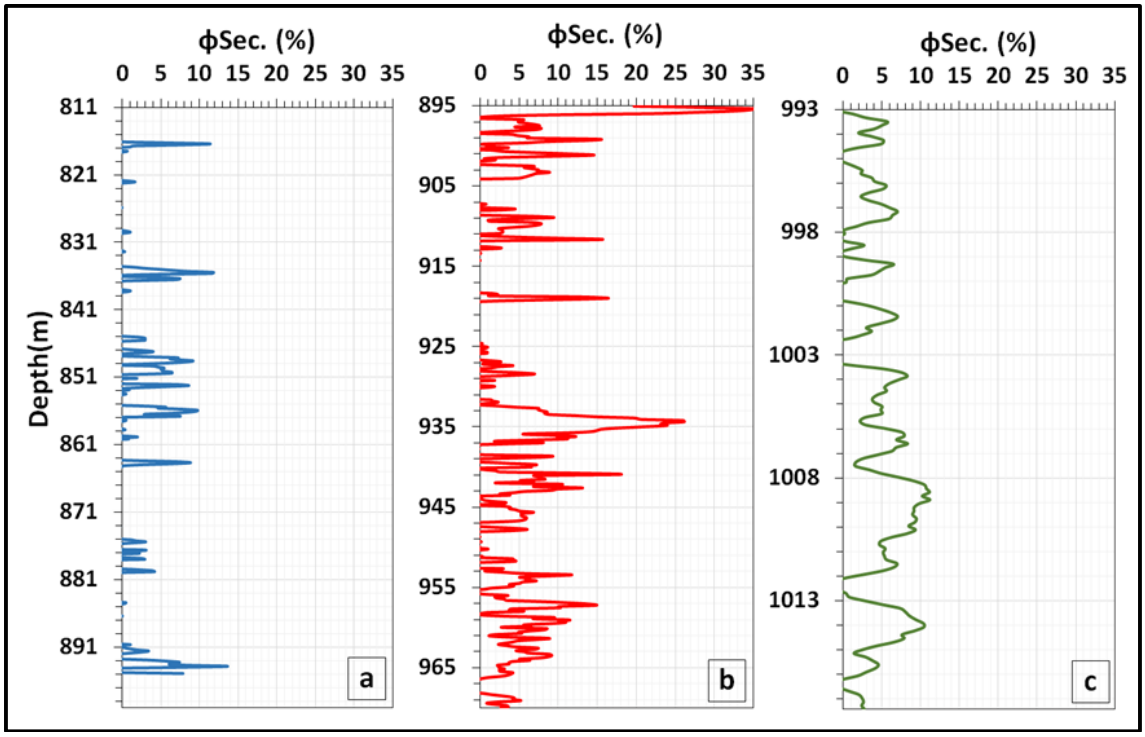

Figure 7. The calculated secondary (fracture) porosity for the Avanah Formation (**a**, Avanah Dense; **b**, Avanah Porous) and **c**, the Khurmala Formation in well KX.

The density and neutron logs are also helpful in the identification of gas zones. Gas in the pores results in an excessively high density porosity (because gas is less dense than water or oil) and an excessively low neutron porosity (because gas contains fewer hydrogen atoms than water or oil) (Asquith & Krygowski, 2004). In the gas-bearing zone, the neutron porosity is less than the density porosity, and the two porosity curves cross over each other. Figure 8 is the plotted crossover curves of the density and neutron porosity for the Avanah and Khurmala Formations. Gas zones are expected to exist in the upper part of the Avanah Dense as appears from the curve's pattern. It’s important to mention that gas saturation has a qualitative relationship with

the crossover's magnitude (the distance between the separated curves); however, the formation pressure has a stronger (again qualitative) impact on the crossover. Whether at shallow depths or exhausted from production, low-pressure zones typically exhibit significant crossover (Asquith & Krygowski, 2004).

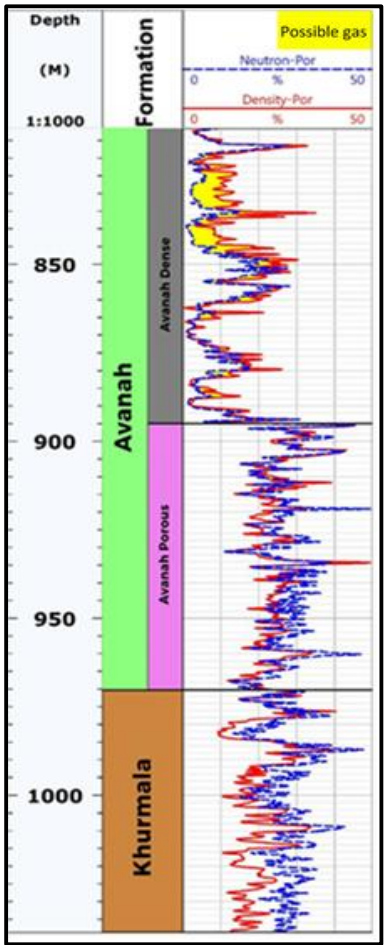

Figure 8. Density -Neutron Crossover for detecting gas zones for the Avanah and Khurmala formations in well KX.

5.4. Water and hydrocarbon saturations

The recorded resistivity of the flushed zone (R_{xo}), the true resistivity of the uninvaded zone (R_t), as well as the resistivity of the transition zone for the Avanah and Khurmala formations are shown in Figure 9. Water saturation for the uninvaded (S_w) and invaded zones (S_{xo}) for the studied section has been calculated by applying equations 5 and 6. The hydrocarbon saturation (S_{hc}), residual hydrocarbon saturation (S_{hcr}), and movable hydrocarbon saturation (S_{hcm}) were then calculated using equations 14 – 16.

$$S_{hc} = 1 - S_w \tag{14}$$

$$S_{hcr} = 1 - S_{xo} \tag{15}$$

$$S_{hcm} = S_{hc} - S_{hcr} \quad (16)$$

By multiplying their saturations and porosity, the bulk volume of water (BVW), residual hydrocarbon (BVRH), and moveable hydrocarbon (BVMH) for the Avanah and Knurmala formations in well KX were computed and shown as illustrated in Figure 10.

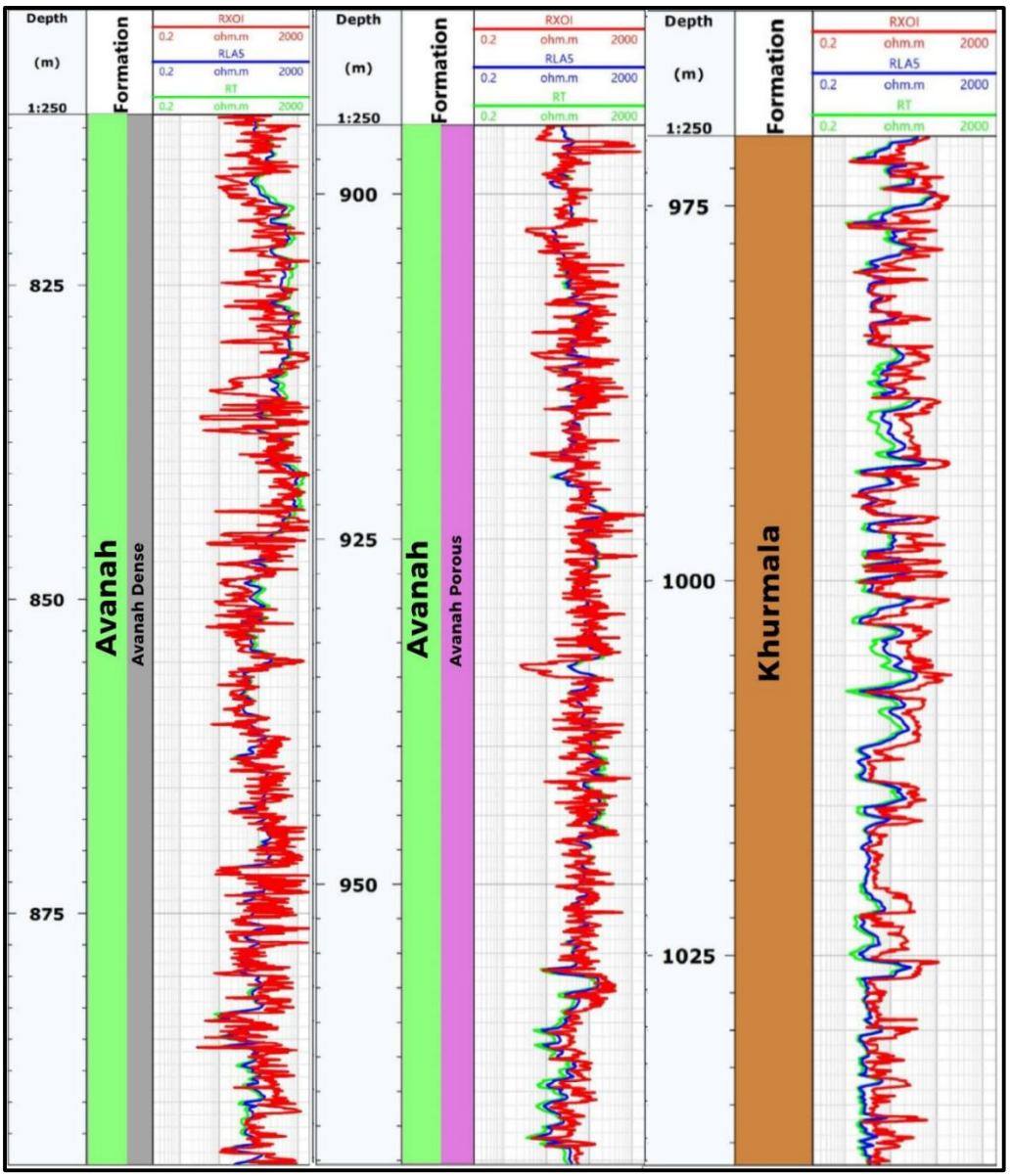

Figure 9. The recorded flushed zone resistivity (Rxo), the transition zone resistivity (Ri, RLA5), and the true resistivity of the uninvaded zone (Rt) for the Avanah and Khurmala formations in well KX.

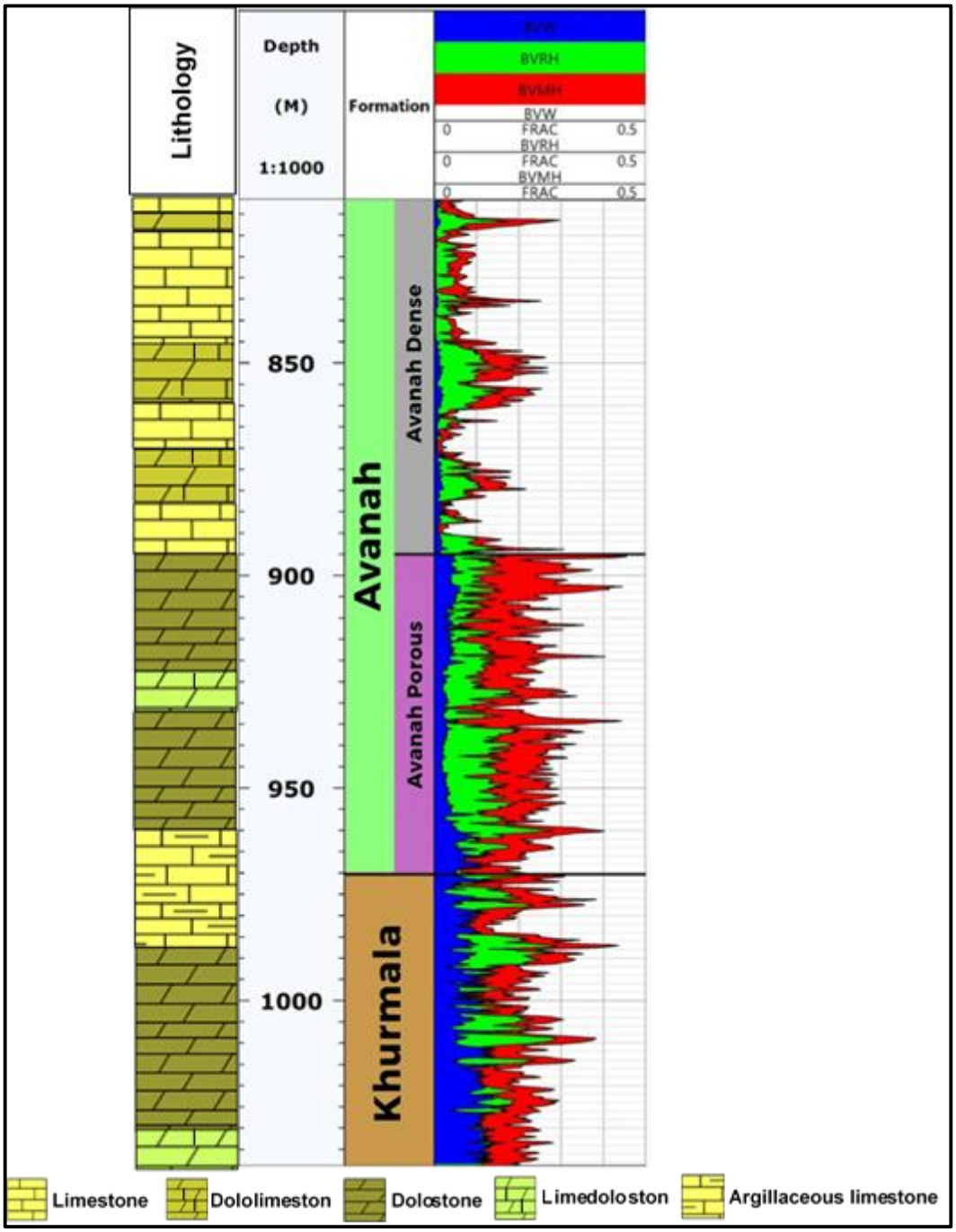

Figure 10. The calculated bulk volumes of water (BVW), residual hydrocarbon (BVRH), and movable hydrocarbon (BVMH) for the Avanah and Khurmala formations in well KX.

Hydrocarbons in various saturations appear to be present across the entire section under study. High proportions of the hydrocarbons in the Avanah Dense, at the upper part of the Avanah Formation, are immobile, most likely due to low permeability and low porosity (small pore spaces).

There is a noticeable amount of movable hydrocarbons in the lower part of the Avanah Formation (Avanah Porous) and the Khurmala Formation. The hydrocarbons are nearly entirely

movable in a number of zones, particularly in the lower Khurmala Formation. From the top of the Avanah Formation to the base of the Khurmala Formation, there is a noticeable and steady rise in water saturation, without the expectation of oil-water contact in the Khurmala Formation.

5.5. Permeability calculation

Neither core analysis data nor Nuclear Magnetic Resonance log (NMR) was available for this study. Therefore, the empirical equation proposed by Coats & Denoo (1981) (Equation 17) is applied to obtain permeability values for a selected depth interval within the studied section, which is believed to be at irreducible water saturation.

The obtained permeability values for the selected depth interval are then used as dependent values in the multilinear regression (MLR) method to find the best equation that represents their relationship with the independent values of the gamma-ray, sonic, neutron, and density logs.

$$K = [100\emptyset^2(1 - Swirr)/(Swirr)]^{½} \quad (17)$$

Where: K: Permeability. Ø: Porosity. S_{wirr}: Irreducible water saturation

The best equation that represented the fluctuation in the mentioned log values and permeability values based on Coats & Denoo's (1981) equation is believed to be Equation 18.

$$K = 83.19663 - (4.2005 \times Gamma\ ray) + (0.175893 \times \Delta t) - (19.215 \times \emptyset N)(824.7657 \times \rho B) \quad (18)$$

Figure 11 is the calculated permeability values for the Avanah and Khurmala Formation applying Equation 18 for the entire studied section.

The upper part of the Avanah Formation (Avanah Dense) showed an obvious anisotropy in permeability. Tight zones with less than 0.1 mD permeability to zones of about 3000 mD can be seen in the Avanah Dense. The highest permeability exists in the depth interval from 845 to 865 m, which also showed distinctive porosity reaching more than 20% with the existence of fractures (Figure 7a).

The permeability in the majority of the Avanah Porous seemed to be very good, reaching a few thousand millidarcies. The formation's bottom, where it meets the Khurmala Formation, has the comparatively lowest permeability (less than 1000 mD).

The Khurmala Formation is also of very good permeability, ranging between 200 and a few thousand millidarcies and being relatively lowest near its contact with the Avanah Formation.

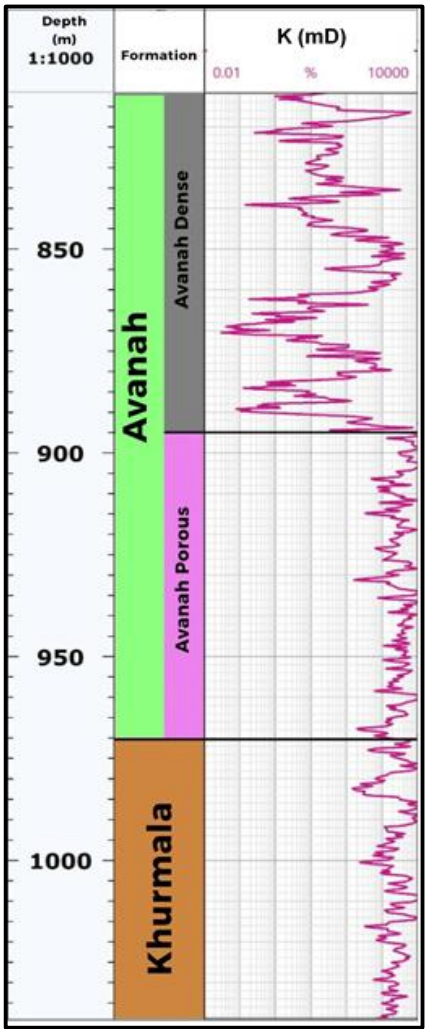

Figure 11. The calculated permeability applying Coats & Denoo's (1981) equation and MLR method for the Avanah and Khurmala formations in well KX.

5.6. Reservoir Units

Based on the variations in the shale content, porosity, permeability, and water saturations, the studied Avanah and Khurmala formations have been subdivided into a number of distinctive primary and secondary reservoir units, as shown in Figure 12. The properties of each reservoir unit are listed in Table 1.

The Avanah Formation is divided into six main reservoir units, starting with reservoir unit 1(RU-A1) at the base of the formation. Among the three reservoir units of the Avanah Porous part of the Avanah Formation, RU-A2, with a thickness of about 35 m, is of highest reservoir properties, whereas RU-A1, with the highest average water saturation (37%) and lowest average porosity and permeability (20.94% and 1918 mD, respectively) is considered to be of the lowest reservoir properties in the Avanah Porous.

The upper part of the Avanah Formation (Avanah Dense) is also divided into three main reservoir units. The reservoir unit RU-A4, with a thickness of about 34 m, is further subdivided

into three secondary reservoir units because of minor variations in the reservoir properties within this unit. RU-A4 is considered to be of the lowest reservoir properties in the entire Avanah Formation in well KX, followed by RU-A6 with a thickness of 33.68 m at the top of the formation, and then RU-A5 in the middle part of the Avanah Dense.

Two main reservoir units were distinguished in the Khurmala Formation. RU-K1, with a thickness of 44.64 m at the lower part of the formation, showed good porosity and permeability, but with a relatively high water saturation rate compared to the other reservoir units. RU-K2, with a thickness of about 22 m, is further subdivided into three secondary reservoir units, among which RU-K2B showed the highest average water saturation (47%) and the lowest average porosity and permeability (18.36% and 1397.5 mD, respectively).

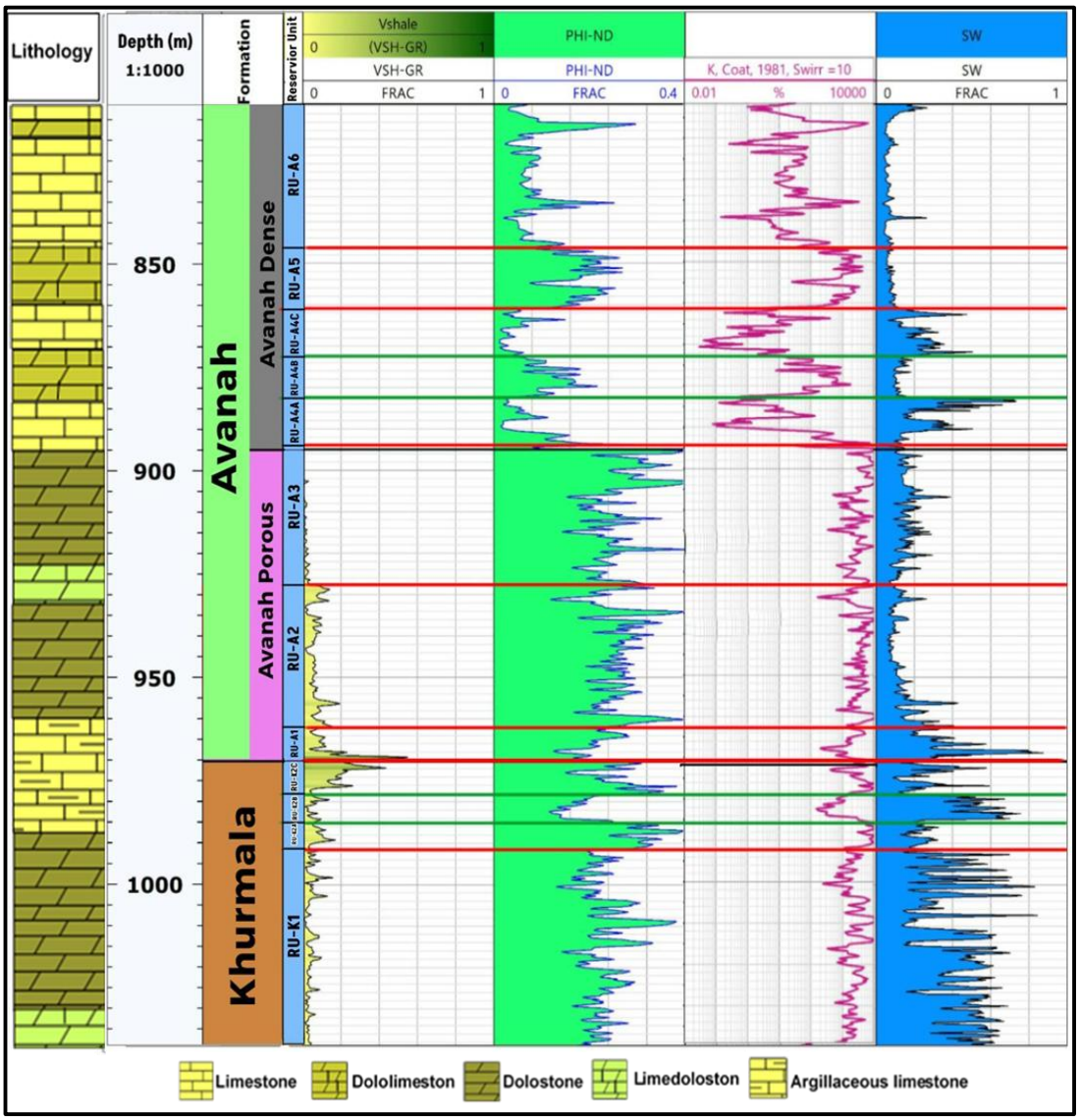

Figure 12. The identified reservoir units for the Avanah and Khurmala formations in well KX are based on variations in the shale content, porosity, permeability, and water saturation.

Table 1. The notable reservoir units of the Avanah and Khurmala formations in well KX, including their average shale content, porosity, permeability, and water saturation values.

Well	Formation		RU	Depth (m)	Thickness (m)	Av. Vsh (%)	Av. $Ø_{NDcorr}$ (%)	Av. K (mD)	Av. Sw (%)
KX	Avanah	Avanah Dense	RU-A6	811.53	33.68	0.015	11.41	242.31	7.37
			RU-A5	845.21	16	0	17.82	1203.21	7.77
			RU-A4C	861.21	11.43	0.244	4.01	16.47	23.48
			RU-A4B	872.64	10.06	0	11.86	305.54	12.27
			RU-A4A	882.7	12.65	0.0168	8.42	536.40	26.73
		Avanah Porous	RU-A3	895.35	32.3	1.07	26.08	5309.71	26.08
			RU-A2	927.65	35.06	6.99	26.13	4715.22	13.45
			RU-A1	962.71	7.46	15.23	20.94	1918.01	37.88
	Khurmala		RU-K2C	970.17	7.62	19.94	25.85	4593.77	25.85
			RU-K2B	977.79	7.47	5.54	18.36	1397.55	47.73
			RU-K2A	985.26	7.01	7.95	30.97	8909.68	23.50
			RU-K1	992.27	46.64	0.03	23.01	2852.16	43.95

5.7 Hydrocarbon movability

Detecting the effectiveness of the fluid's movability within reservoirs is vital for best evaluating the production capacity. There are several techniques by which the movability of fluids can be detected within reservoirs based on the wireline log data. The Flow Zone Indicator (FZI) technique proposed by Amaefule et al. (1993) is very helpful in differentiating between the different Hydraulic Flow Units (HFU) that have different permeability to porosity ratios, regardless of the type of fluid. Movable Hydrocarbon Index (MHI), on the other hand, is another technique that aids in distinguishing zones of effective movable hydrocarbons.

The calculation of the FZI values, as proposed by Amaefule et al. (1993), needs firstly values for the reservoir quality index (RQI) and normalized porosity (Øz), which can be obtained by equations 19 – 21.

$$RQI = 0.0314\ (\mathrm{K}/Ø)^{½} \tag{19}$$

$$Øz = Øe/(1 - Øe) \tag{20}$$

$$FZI = RQI/Øz \tag{21}$$

From the cumulative distribution of the calculated FZI values for the Avanah and Khurmala formations in well KX, four distinguished hydraulic flow units were identified representing FZI range values between 3.28 and 29 µm (Figure 13).

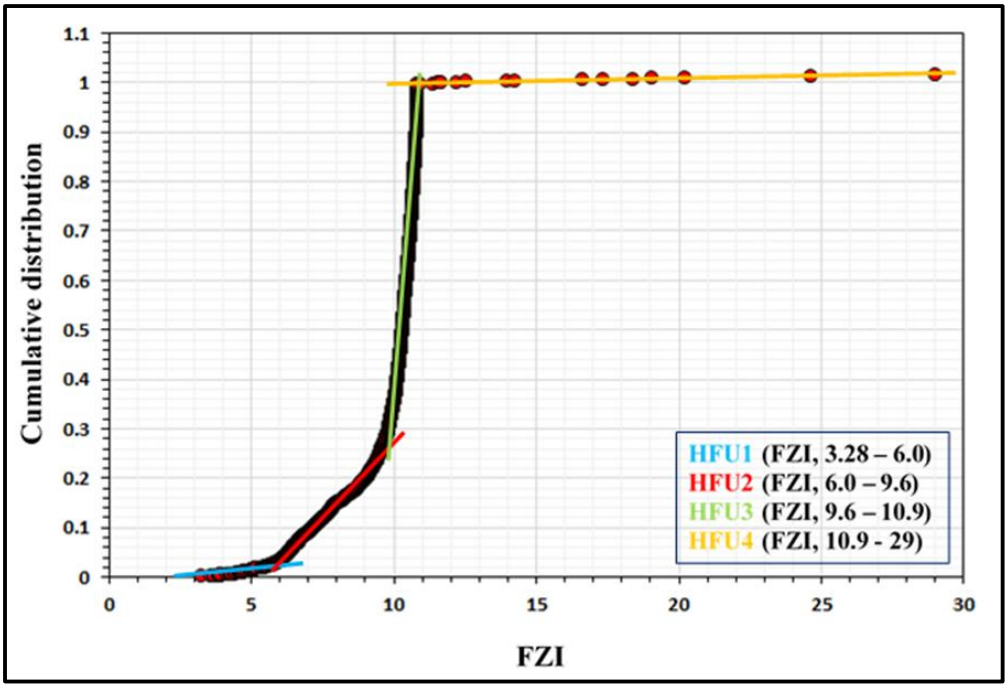

Figure 13. Cumulative distribution of the calculated FZI values for the Avanah and Khurmala formations in well KX.

Evaluation of the reservoir quality for the Avanah and Khurmala formations, depending on their calculated RQI and FZI as proposed by Fea et al. (2022), based on the classification ranks suggested by Nabawy et al. (2018), revealed that HFU3 is the best of the four identified hydraulic flow units, with good FZI resulting from very good RQI values (Figure 14).

Although HFU4 is of highest and good FZI value, its RQI is considered tight to fair, which is most probably due to low porosity and permeability.

The HFU2 is also of good FZI values, ranging between 9.6 and 10.9, with a wide range of RQI values representing a tight to good reservoir quality zone with high heterogeneity. Zones of lowest reservoir quality are those representing HFU1, whose FZI are fair to good with (less than 6 µm and tight to poor RQI).

The distribution of the identified HFUs along the studied section is shown in Figure 15.

The wide range of the flow capacity in the upper part of the Avanah Formation (Avanah Dense) indicates high heterogeneity of the lithology of this part of the formation Barzanji et al., 2023).

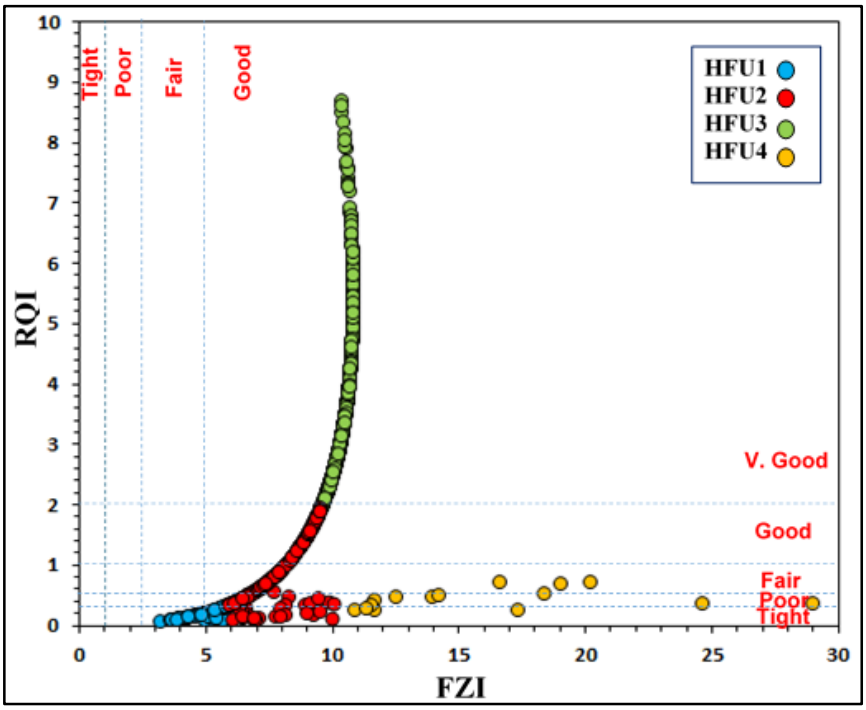

Figure 14. FZI versus RQI to show the reservoir quality based on the classification ranks suggested by Nabawy et al. (2018) for the studied section in well KX (after Fea et al., 2022).

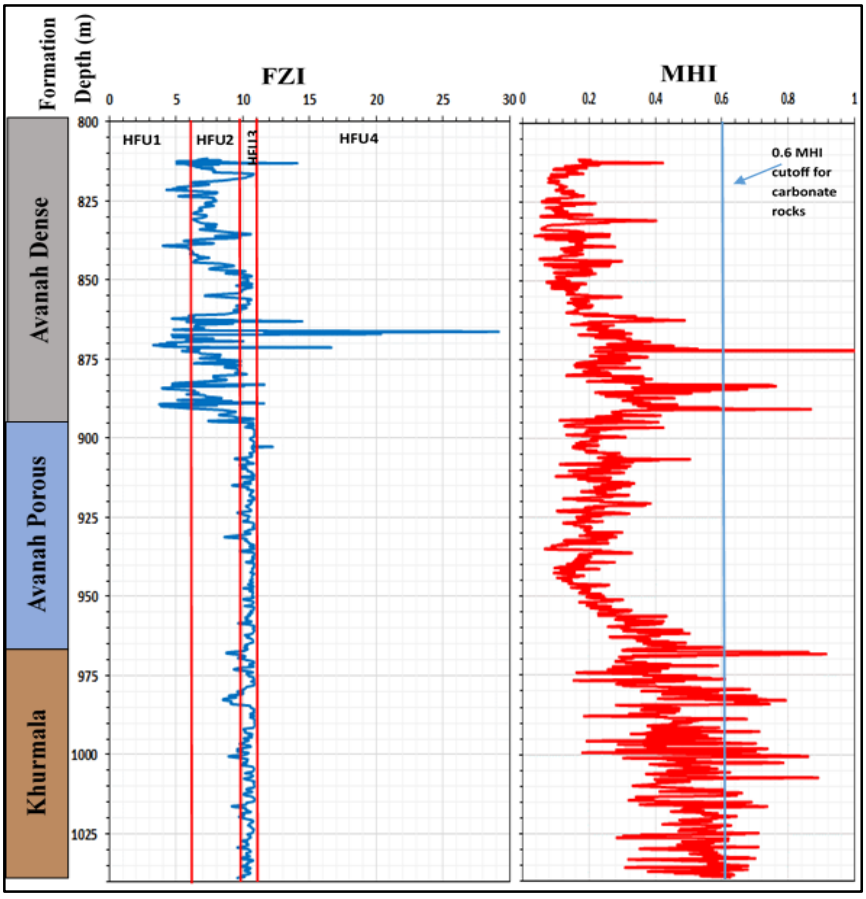

Figure 15. The calculated FZI values and the identified HFUs for the Avanah and Khurmala formations in well KX, along with their calculated MHI value.

The lower part of the Avanah Formation (Avanah Porous) and the Khurmala Formation are homogeneous to an appreciable degree, as appears from their FZI values, which are entirely of one HFU (HFU3), which is also the best one among the identified four.

The same technique was recently used by Baban & Saeed (2025) to qualitatively characterize the hydraulic flow units of the Miocene Jeribe Formation in the northern Iraqi oilfield of Hamrin.

As the FZI technique defines the flow capacity of fluids without distinguishing between water or hydrocarbon movability, the technique of MHI has been applied to identify the zones of movable hydrocarbons along the studied Avanah and Khurmala formations. MHI is the ratio of Sw/Sxo, and the smaller the value of this ratio, the greater the ability of the hydrocarbon to move.

According to Schlumberger (1972), in carbonate reservoirs, whenever the MHI value is less than 0.6, movable hydrocarbons are indicated. As shown in Figure 14, except for three narrow horizons in the Avanah Dense, almost the entire Avanah Formation contains effective movable hydrocarbons. The Khurmala Formation, on the other hand, showed a lot of horizons with ineffective hydrocarbon movability, intercalated horizons with effective movable hydrocarbons.

The difference between the hydrocarbon movability indicated by Archi equation and the MHI is that by the MHI method, only those intervals considered bearing movable hydrocarbons whose S_{xo} values are greater by at least 40% of their S_w, while by the Archie method, any excess of S_{xo} over the S_w, regardless of the value, is an indication of the existence of movable hydrocarbons.

6. Conclusions

From the analysis of the available wireline log data for the Avanah and Khurmala formations in well KXof the Khurmala Oilfield, it was concluded that the upper part of the Avanah Formation (Avanah Dense) is mostly limestone and some dololimestone, while the lower part (Avanah Porous) and the Khurmala Formation are mainly made up of dolostone and limedolostone. The Avanah Dense is almost clean and free of shale, while shaly and shale intervals often occur in the Avanah Porous and the Khurmala Formation, particularly in depth intervals near their contacts. The shale within the Avanah Porous and the Khurmala Formation appears to have a primarily laminated and dispersed distribution type, alongside structural types in a few horizons. The average porosity in the Avanah Dense is around 10.7%, in the Avana porous is 24.38%, and in the Khurmala Formation is about 24.54%. Secondary (fracture) porosity contributed effectively to increasing the total porosity of the Avanah Porous and of the Khurmala Formation. Water saturation is progressively rising from the top of the Avanah Formation towards the base of the Khurmala Formation, and hydrocarbons are present across the entire examined section. A sizable portion of the current hydrocarbons is regarded as residual. Permeability of the lower part of the Avanah Formation (Avanah Porous) is very good,

reaching a few thousand millidarcies and being relatively lower near its contact with the Khurmala Formation, while the permeability of Avanah Dense ranges between negligible in the tight zones to very good (about 3000 mD) in some porous zones. The Khurmala Formation also has very good permeability, ranging between 200 and a few thousand millidarcies. Based on the variations in the shale content, porosity, permeability, and water saturations, the Avanah Formation can be divided into six main reservoir units, and the Khurmala Formation into two. The fluids, based on the calculated FZI values, are flowing in four distinctive hydraulic units. The Avanah Porous and the Khurmala Formation are seen as being homogenous and of good to very good flow capacity compared to the Avanah Dense, which includes zones of a wider range of flow capacity between tight and very good. The Avanah Formation primarily consists of effective movable hydrocarbons, whereas many horizons in the Khurmala Formation contain ineffective or no movable hydrocarbons.

Acknowledgment

The authors express their deep gratitude to the Operated Oil Company in the Iraqi Kurdistan Region for providing the log data used in this study.

References

Abdula, R. A., Hussein, H. S., Hamad, M. S., & Abdulla, A. M. (2024). Reservoir Characterization of the Paleogene Khurmala Formation in Tawke and Shaqlawa Areas, Kurdistan Region of Iraq. *The Iraqi Geological Journal*, 62–77. https://doi.org/10.46717/igj.57.1C.5ms-2024-3-17

Abdullah M. A., Faris N. H., & Abdulsalam. M. S. (2020). Microfacies and Palaeoenvironment of Avanah Formation (Middle Eocene), Geli Bessri in Dohuk City / North of Iraq. *Tikrit Journal of Pure Science*, *25*(1), 85–93. https://doi.org/10.25130/tjps.v25i1.217

Abid, A. A., Salih, N. M., & Martyushev, D. A. (2023). Paleoenvironmental Evaluation Using an Integrated Microfacies Evidence and Triangle Model Diagram: A Case Study from Khurmala Formation, Northeastern Iraq. *Journal of Marine Science and Engineering*, *11*(11), 2162. https://doi.org/10.3390/jmse11112162

Ahmed, A. M. (2022). Microfacies Analysis and Depositional Environment of Khurmala Formation (Paleocene-Early Eocene) in Kalati Section, Akre Area, Kurdistan Region, Iraq. *The Iraqi Geological Journal*, 105–117. https://doi.org/10.46717/igj.55.1D.7Ms-2022-04-23

Akbar, M., Vissapragada, B., Alghamdi, A. H., Allen, D., & Herron, M. (2000). A snapshot of carbonate reservoir evaluation. *Oilfield Review*, *12*, 20–40.

Al-Banna, N., Al-Mutwali, M. M., & Al-Ghrear, J. S. (2006). Facies Analysis and Depositional Environment of Khurmala Formation in Bekhair Anticline –Dohuk Area, North Iraq. *Iraqi National Journal of Earth Science (INJES)*, *6*(2), 13–22. https://doi.org/10.33899/earth.2006.36375

Al-Barzanji, Sh. J. (1989). *Microfacies study of the Khurmala Formation from selected sections in north and north-east Iraq*. Salahaddin University.

Al-Dabagh, M. M. (2010). *Facies and Depositional Model of Khurmala Formation (Paleocene- Early Eocene) at selected Exposures from Northern Iraq*. Mosul University.

Al-Ehmeedy, I., Al-Lihaibi, S. F., & Al-Miamary, F. A. (2012). Microfacies analysis and facies model of Khurmala Formation (Upper Paleocene – Lower Eocene), Dokan Area, northeastern Iraq. *Tikrit Journal of Pure Science*, *3*, 186–195.

Al-Eisa, M. E. (1983). *Study of the foraminifera and depositional environment of fossils in the Khurmala Formation, Shaqlawa area*. Mosul University.

AL-Hamdany, A. M., & Sulaiman, M. A. M. (2014). Porosity of Avanah Formation and its Stratigraphical Distribution in Selected Wells of Kirkuk Oil Field. *Iraqi National Journal of Earth Science (INJES)*, *14*(1), 49–66. https://doi.org/10.33899/earth.2014.87488

Al-Lihaibi, S. (2012). Diagenesis of Khurmala Formation in Dokan Area, North Eastern Iraq. *Iraqi National Journal of Earth Science (INJES), 12*(3), 17–34. https://doi.org/10.33899/earth.2012.64507

Al-Qayim, B. (1995). Sedimentary facies anatomy of Khurmala Formation, Northern Iraq. *Iraq Geological Journal*, *28*, 36–46.

Amaefule, J. O., Altunbay, M., Tiab, D., Kersey, D. G., & Keelan, D. K. (1993, October 3). Enhanced Reservoir Description: Using Core and Log Data to Identify Hydraulic (Flow) Units and Predict Permeability in Uncored Intervals/Wells. *SPE Annual Technical Conference and Exhibition*. https://doi.org/10.2118/26436-MS

Aminzadeh, & Dasgupta. (2013). Geophysics for Petroleum Engineers. In *Developments in Petroleum Science* (Vol. 60).

Aqrawi, A., Goff, J., Horbury, A., & Sadooni, F. (2010). *The petroleum geology of Iraq*. Scientific Press.

Asaad, I. S. (2022). Lithostratigraphy & microfacies analysis of Avanah Formation (Middle Eocene) in Gomaspan section, northeast Erbil City, Kurdistan region, Iraq. *Kuwait Journal of Science*, *49*(3). https://doi.org/10.48129/kjs.11183

Asaad, I. S., Al-Haj, M. A., & Malak, Z. A. (2022). Depositional Setting of Khurmala Formation (Paleocene-Early Eocene) in Nerwa section, Berat Anticline, Kurdistan Region, Northern Iraq. *Iraqi Geological Journal*, *55*(1F), 20–39. https://doi.org/10.46717/igj.55.1F.2Ms-2022-06-17

Asaad, I. S., & Balaky, S. M. (2018). Microfacies analysis and depositional environment of Khurmala Formation (Paleocene – Lower Eocene), in the Zenta village, Aqra district, Kurdistan Region, Iraq. *Iraqi Bulletin of Geology and Mining*, *2*(4), 1–15.

Asquith, G., & Krygowski, D. (2004). Methods in Exploration, No. 16. In *Basic relationships of well log interpretation* (pp. 1–20). AAPG (American Association of Petroleum Geologists).

Aziz, N. (2012). On Some Ostracode Species of the Avanah Formation from Dohuk Area, N. Iraq. *Iraqi National Journal of Earth Science (INJES), 12*(2). https://doi.org/10.33899/earth.2012.36303

Baban, D. H., & Ahmed, S. M. (2021). Source Rocks' Potentiality of the Sargelu Formation (Middle Jurassic) in the Taq Taq Oilfield, Kurdistan Region, Iraq. *The Iraqi Geological Journal*, 59–85. https://doi.org/10.46717/igj.54.2E.5Ms-2021-11-21

Baban, D. H., Barzanji, S. S. S., & Ahmed, M. M. (2023). Evaluation of the Shale Impact on Reservoir Characterization, the Jeribe Carbonate Reservoir in an Oilfield Northern Iraq as a Case Study. *Iraqi Geological Journal*, *56*(2). https://doi.org/10.46717/igj.56.2E.14ms-2023-11-19

Baban, D., Qadir, F., & Mohammed, A. (2020). Reservoir Rock Properties of the Upper Cretaceous Shiranish Formation in Taq Taq Oilfield, Iraqi Kurdistan Region. *Journal of Zankoy Sulaimani - Part A*, *22*(1), 363–388. https://doi.org/10.17656/jzs.10799

Baban, D., & Saeed, M. (2025). Lateral Variations in the Reservoir Properties of the Middle Miocene Jeribe Formation in the Allas Dome of the Hamrin Oil Field, Northern Iraq. *Iraqi Bulletin of Geology and Mining*, *21*(1), 207–238. https://doi.org/10.59150/ibgm2101a13

Barzani, A. T., & Al-Qayim, B. (2019). Dolomitization And Porosity Evaluation Of Khurmala Formation, Gara Anticline, Dohuk Area, Kurdistan Region, Iraq. *The Iraqi Geological Journal*, 1–17. https://doi.org/10.46717/igj.52.2.1Ms-2019-12-24

Barzani, B. A. (2016). *Microfacies, depositional environment, and sequence stratigraphy of Avanah Formation from selected sections in Iraqi Kurdistan Region*. Salahaddin University.

Barzanji, S. S., Baban, D. H., & Ahmed, M. M. (2023). Moveability and Nature of the Reservoir Hydrocarbons in the Lower Miocene Jeribe Formation in X-Oilfield, Northern Iraq. *The Iraqi Geological Journal*, 80–92. https://doi.org/10.46717/igj.56.1F.6ms-2023-6-14

Bateman, R. M. (1985). *Open-hole log analysis and formation evaluation*. International Human Resources Development Corporation.

Bellen, R. C., Van, D. H. V., Wetzel, R., & Morton, D. (1959). *Lexique stratigraphique international, Asie (Iraq)* (Vol. 3). International Commission on Stratigraphy.

Burke, J. A., Campbell, R. L., & Schmidt, A. W. (1969, October 30). The Litho-Porosity Cross Plot: A Method Of Determining Rock Characteristics For Computation Of Log Data. *SPE Illinois Basin Regional Meeting*. https://doi.org/10.2118/2771-MS

Coats, G. R., & Denoo, S. (1981). The producibility answer product. *The Technical Review, 29*, 55–144.

Dewan, J. T. (1983). *Modern open hole log interpretation*. Pennwell Publishing Co.

Fea, I., Abioui, M., Nabawy, B. S., Jain, S., Bruno, D. Z., Kassem, A. A., & Benssaou, M. (2022). Reservoir quality discrimination of the Albian-Cenomanian reservoir sequences in the Ivorian basin: a lithological and petrophysical study. *Geomechanics and Geophysics for Geo-Energy and Geo-Resources*, *8*(1), 1. https://doi.org/10.1007/s40948-021-00297-8

Ghorab, M., Ramadan, M. A. M., & Nouh, A. Z. (2008). The Relation Between the Shale Origin (Source or non Source) and its Type forAbu Roash Formation at Wadi El- Natrun Area, South of Western Desert, Egypt. *Australian Journal of Basic and Applied Sciences*, *2*(3).

Halliburton, A. D. (2001). *Basic petroleum geology and log analysis*. Halliburton Company.

Jassim, S. Z., & Buday, T. (2006). Units of the stable shelf. In In S. Z. Jassim & J. C. Goff (Eds.) (Ed.), *Geology of Iraq* (pp. 53–72). Dolin.

Kargarpour, M. A. (2020). Carbonate reservoir characterization: an integrated approach. *Journal of Petroleum Exploration and Production Technology*, *10*(7), 2655–2667. https://doi.org/10.1007/s13202-020-00946-w

Karim, Ch. A. (2009). *Stratigraphical and Paleontological Study of Khurmala Formation (Paleocene – Lower Eocene) in Shaqlawa Area -Northern Iraq*. Mosul University.

Karim, K. H., Daoud, H. S., & Kuradawy, A. R. H. (2018). Record Of Khurmala Formation (Late Paleocene – Early Eocene) In The Sulaimaniah Governorate, Kurdistan Region, Northeast Iraq. *The Iraqi Geological Journal*, 34–55. https://doi.org/10.46717/igj.51.1.3Ms-2018-06-25

Khalaf, S. K., & Aziz, N. M. (2009). On some species of the Ostracode genera Cytherella, Bairdia, and Bairdoppilata from Avanah Formation, Dohuk Area, Northern Iraq. *Tikrit Journal of Pure Science*, *3*(14).

Larionov, W. W. (1969). *Radiometrija Skwaschin*. Nedra Verlag.

Mamaseni, W. J., Asaad, I. Sh., & AL-Juboury, A. I. (2024). Reservoir characteristics of the middle Eocene Avanah Formation in Erbil governorate, northern Iraq: Integration of outcrop and subsurface data. *Bulletin Of The Mineral Research and Exploration*, 1–2. https://doi.org/10.19111/bulletinofmre.1453586

Moradi, S., Moeini, M., Ghassem al-Askari, M. K., & Mahvelati, E. H. (2016). Determination of Shale Volume and Distribution Patterns and Effective Porosity from Well Log Data Based On Cross-Plot Approach for A Shaly Carbonate Gas Reservoir. *IOP Conference Series: Earth and Environmental Science*, *44*, 042002. https://doi.org/10.1088/1755-1315/44/4/042002

Musheer, S. H. (2021). *Petrophysical assessment of Avanah reservoir in Khurmala dome of the Kirkuk Field, Iraq*. Near East University.

Nabawy, B. S., Basal, A. M. K., Sarhan, M. A., & Safa, M. G. (2018). Reservoir zonation, rock typing and compartmentalization of the Tortonian-Serravallian sequence, Temsah Gas Field, offshore Nile Delta, Egypt. *Marine and Petroleum Geology*, *92*, 609–631. https://doi.org/10.1016/j.marpetgeo.2018.03.030

NOC. (1994). *The annual report about the reservoirs for the year 1993*.

North, F. K. (1985). *Petroleum geology*. Allen & Unwin Inc.

O'Brien, N. R. (1996). Shale lamination and sedimentary processes. *Geological Society, London, Special Publications*, *1*(116), 23–36.

Omer, M. F., Omer, D., & Zebari, B. G. (2014). High resolution cathodoluminescence spectroscopy of carbonate cementation in Khurmala Formation (Paleocene-L. Eocene) from Iraqi Kurdistan Region, Northern Iraq. *Journal of African Earth Sciences*, *100*. https://doi.org/10.1016/j.jafrearsci.2014.06.016

Rashid, F., Hussein, D. O., & Zangana, H. A. (2020). Petrophysical Investigation of the Khurmala Formation in Taq Taq Oil Field, Zagros Folded Belt. *Aro - The Scientific Journal Of Koya University*, *8*(1), 5–16. https://doi.org/10.14500/aro.10556

Schlumberger. (1972). *Log interpretation manual: Principles* (Vol. 1). Schlumberger Well Services Inc.

Schlumberger. (1979). *Log interpretation charts*. Schlumberger Limited.

Schlumberger. (1989). *Log interpretation principles/applications*. Sugar Land, TX.

Schlumberger. (2019). *Technical challenges—carbonate reservoirs.*

Sharbazheri, K. M., & Abawi, T. S. (1987). Larger foraminifera from the Avanah Formation (Middle Eocene) of the Dhouk area, Northern Iraq. *Journal of Geological Society*, *20*, 70–88.

Thomas, E. C., & Stieber, S. J. (1975). The distribution of shale in sandstones and its effect upon porosity. *SPWLA 16th Annual Logging Symposium 1975*.

Yang, L. (2015). *A Petrophysical Evaluation of the Trenton-Black River Formation of the Michigan Basin*. Michigan Technological University.

About the authors

Shiraz K. Birezhy graduated from the Department of Geology at the University of Salahaddin in 2021. In 2024, Shiraz joined the M.Sc. Program in the Department of Earth Sciences and Petroleum at the University of Salahaddin, works for one of the well-known oil companies in the Iraqi Kurdistan Region, specializing in petroleum geology.

e-mail: shirazkafi@gmail.com

Dler H. Baban (Ph.D.) is a professor of petroleum geology at the Department of Earth Sciences and Petroleum at the University of Sulaimani. Dler gained his MSc in general geology from the Department of Geology/University of Baghdad in 1989 and his Ph.D. in petroleum geology in 1996 from the same department. Dler supervised a number of M.Sc. and Ph.D. students in petroleum geology specifications and worked as a consultant for the FAO organization and for a number of foreign oil companies in the Iraqi Kurdistan Region.

e-mail: dler.mohamad@univsul.edu.iq